

# Dynamic Recrystallization in Pure Magnesium

Oleg Sitdikov and Rustam Kaibyshev

Microstructural evolution of commercial grade pure magnesium was studied during plastic deformation by torsion under high pressure at ambient temperature and by compression at temperatures ranging from 293 to 773 K and at a strain rate of  $3 \times 10^{-3} \text{ s}^{-1}$ . Grain refinement takes place by operation of dynamic recrystallization (DRX) at all examined temperatures. The mechanisms of DRX change with temperature and strain. As a result, unusual dependencies of recrystallized grain size against strain and recrystallized volume fraction against temperature are observed. In the temperature interval of 293–623 K the deformation twinning results in “twin” mechanism of DRX, which processes strain softening at an initial stage of deformation. At  $T \leq 423 \text{ K}$  the other mechanism of low temperature DRX takes place at high strains. Such DRX is accompanied by strain hardening. In contrast, continuous DRX (CDRX) yielding a steady-state flow operates frequently at temperatures ranging from 523 to 773 K. CDRX occurs mainly in overall recrystallization process at elevated temperatures. Discontinuous DRX (DDRX) takes place by bulging of boundaries of coarse recrystallized grains evolved from twins at  $T = 723 \text{ K}$ . DDRX occurs repetitively, but gives an insignificant contribution into total recrystallization process. The present results suggest that the mechanisms of DRX and the deformation mechanisms are closely related.

## 1. Introduction

Magnesium alloys are expected to be one of the most promising structural materials for application in aerospace, automotive and railway industry in as much they have low density, which can directly and substantially reduce vehicle weight. In addition, magnesium alloys exhibit good damping characteristics, dimensional stability, machinability and low costs, *etc.* However, these alloys exhibit poor workability owing to the lower symmetry, and it restricts their commercial application as wrought materials. As a result, about 85 pct of commercial applications of magnesium alloys fall on cast materials. In order to increase the benefits of magnesium alloys, it is important to improve their workability up to value which can allow effectively producing complex engineering components directly from wrought products. Thermomechanical processing (TMP) is an attractive procedure to improve workability in hot and warm working conditions. An important process occurring during TMP of magnesium alloys is dynamic recrystallization (DRX).<sup>1,2)</sup>

DRX can play a role of softening process, and results in increased plasticity resource.<sup>1)</sup> Studies of DRX have contributed essentially to improve manufacturing processing. Examination of microstructural evolution in magnesium under deformation may provide a better understanding of the DRX process taking place in materials with low crystal symmetry. However, DRX in magnesium and its alloys was poorly examined.<sup>2,3)</sup> There is still a lack of the understanding of some important aspects of DRX in magnesium.

Mechanism of DRX in a low alloy magnesium was found to involve dynamic polygonization in rotated lattice regions adjacent to initial boundaries.<sup>2)</sup> Following gradual conversion of subboundaries into high-angle boundaries results in the formation of recrystallized grains along original boundaries. This mechanism of grain formation is continuous recrystallization (CDRX), which normally occurs in materials with high stacking fault energy (SFE).<sup>4)</sup> CDRX in magnesium with

low SFE, *e.g.* 10 to 40 MJ/m,<sup>2,5,6)</sup> has not been yet explained. It is known<sup>1)</sup> that DRX proceeds by nucleation followed by growth. Dynamic nucleation rate in magnesium is the slowest process<sup>3)</sup> and can control the recrystallization. Nucleation in cubic metals with low to medium SFE can occur frequently by bulging<sup>7,8)</sup> or twinning<sup>9)</sup> in addition to subgrain formation. However, these nucleation mechanisms have not been reported for magnesium.

The aim of the present paper is to review the recent works on DRX in commercial grade magnesium (99.9 mass%Mg). Recrystallization behavior of the magnesium will be summarized in detail. The DRX mechanisms operating in a wide temperature range of 293–773 K and at a strain rate of about  $10^{-3} \text{ s}^{-1}$  will be discussed. A specific attention will be paid to the link between microstructural evolution and operating deformation mechanism.

## 2. Mechanical Behavior

Typical true stress-true strain curves for the magnesium at various temperatures ranging from 423 to 773 K and at a fixed strain rate of  $3 \times 10^{-3} \text{ s}^{-1}$  are shown in Fig. 1(a).<sup>10)</sup> Two types of the  $\sigma - \varepsilon$  curves can be distinguished. At  $T = 423\text{--}623 \text{ K}$  a well-defined stress peak is observed. An extensive strain hardening is followed by a strain softening at initial stage of plastic deformation. A steady-state deformation is observed after a strain of about 0.5. The strain at a stress peak (the peak strain,  $\varepsilon_{\text{peak}}$ ) and the steady-state strain,  $\varepsilon_{\text{ss}}$ , tend to decrease with increasing temperature. The ratio between the peak stress,  $\sigma_{\text{peak}}$ , and the steady-state flow stress,  $\sigma_{\text{ss}}$ , decreases from 1.5–1.9 at  $T = 423\text{--}523 \text{ K}$  to 1.3 at  $T \geq 573 \text{ K}$ . In the temperature range 673–773 K the steady-state flow is attained after a small strain of about 0.02. No stress peak is clearly observed at these temperatures.

The microhardness of specimens deformed by torsion straining under high pressure at ambient temperature is shown as a function of strain in Fig. 1(b).<sup>11)</sup> The microhardness in unrecrystallized areas at  $\varepsilon = 0.5$  is about 50 pct higher than

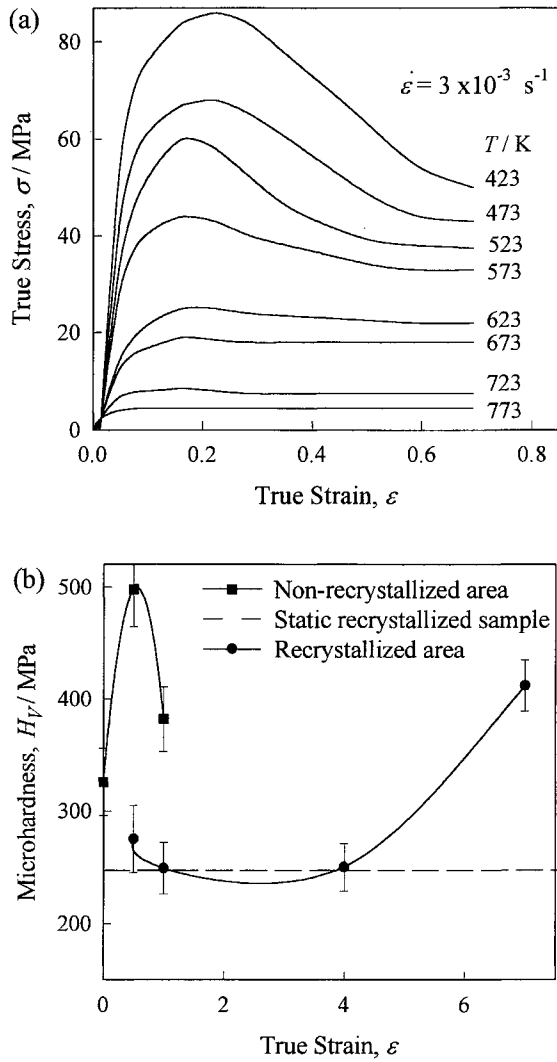


Fig. 1 (a)  $\sigma - \epsilon$  curves at various temperatures at an initial strain rate of  $3 \times 10^{-3} \text{ s}^{-1}$ . (b) Strain dependence of microhardness for magnesium deformed at ambient temperature.

that in the initial state. Further straining yields an abrupt reduction in the microhardness. Microhardness at strains of  $\epsilon = 2-4$  approaches that of statically recrystallized magnesium. At  $\epsilon > 4$ , however, an extensive strain hardening takes place again.

### 3. Microstructure Evolution

Initial microstructure of the magnesium consisted of coarse grains with an average size of 2 mm. Twins belonging to one system presented in grain interiors. Twin fraction is about 12 pct of the material volume, and an average width of twin lamellas was about  $8 \mu\text{m}$ .<sup>10,12</sup> The microstructures developed during deformation in the three different temperature intervals can be divided into the following three distinct categories. Here microstructural evolution will be considered at ambient temperature, 573 and 723 K.

#### 3.1 Ambient temperature

Plastic deformation at room temperature yields an extensive twinning on multiple systems<sup>11,12</sup> (Fig. 2) and the for-

mation of dense dislocation pile-ups within initial grains. The latter results in increase of lattice dislocation density and internal elastic strain in the strain interval of 0–1.<sup>11</sup> The volume fraction of twined areas increases up to 45 pct at  $\epsilon = 0.5$  and 85 pct at  $\epsilon = 1$  (Fig. 2). The average width of deformation twins was found to be  $2.5 \mu\text{m}$  and  $4.5 \mu\text{m}$  at  $\epsilon = 0.5$  and  $\epsilon = 1$ , respectively. This suggests that growth of twin lamellas takes place during deformation. Two processes result in the formation of crystallites surrounded by twin boundaries.<sup>11,12</sup> One of them is the mutual intersection of primary twins. In addition, the secondary twinning occurs within coarse lamellas of primary twins. As a result, the subdivision of primary twins by secondary twins takes place. These crystallites can serve as nuclei and the formation of chains of recrystallized grains evolved at the sites of former twins. This process of microstructural evolution is called as “twin DRX (TDRX)”.<sup>12</sup> Recrystallized grains are first evolved after  $\epsilon = 0.5$  (Fig. 3). An extensive migration of former twin boundaries takes place during following deformation and results in increase of recrystallized grain sizes and their volume fraction (Fig. 3). After  $\epsilon = 4$ , such grains are fully developed in a whole volume (Fig. 2). Notably the dislocation densities inside the twin recrystallized grains ( $\rho = 10^{12} \text{ m}^{-2}$ ) are significantly less than those in unrecrystallized areas ( $\rho = 3 \times 10^{15} \text{ m}^{-2}$ ), and grain boundaries exhibit well-defined extinction contours (Fig. 2). As a result, a dramatic drop in internal elastic strain is observed in the strain interval of 1–4.

No twinning occurs in a fine grain structure evolved during following deformation. Repetitive DRX occurs within these twin grains and results in the formation of new grains<sup>11</sup> (Fig. 2). Recrystallized grain sizes in the second generation is 4–5 times smaller than those of twin grains (Fig. 3). These grains contain high dislocation density<sup>11</sup> ( $\rho = 2 \times 10^{14} \text{ m}^{-2}$ ) (Fig. 2). In addition, these grain boundaries usually exhibit a specific contrast, which suggests high density of grain boundary dislocations.<sup>13</sup> As a result, a significant increase in internal elastic strain takes place in the strain interval of 4–7.<sup>11</sup> This type of DRX may be called as “low temperature DRX (LTDRX)”.<sup>11</sup> Notably the similar sequence of microstructural evolution takes place in the temperature interval of 423–473 K (Fig. 5(a)). Therefore, this type of microstructural evolution can be inherent in cold deformation range of magnesium.<sup>15–17</sup>

#### 3.2 Intermediate temperature

At  $T = 573 \text{ K}$ , TDRX begins to operate extensively at strains less than the steady-state strain,  $\epsilon_{ss}$ . Deformation twinning on multiple systems results in increase of volume fraction of twins up to 60% at a strain of about 0.1 (Fig. 4). The average width of deformation twins was about  $8 \mu\text{m}$ .<sup>10,12</sup> Nucleation in twin lamellas occurs by similar ways as that at room temperature (Fig. 4). The formation of secondary twins within lamellas of primary twins plays an important role in TDRX at this temperature (Fig. 4(b)). In addition, subdivision of coarse twin lamellas by transverse subboundaries takes place (Fig. 4(c)). As a result, the extensive formation of nuclei exhibiting rectangular shape occurs (Fig. 4(a)). Their size is determined by width of twin lamellas. With increasing strain the formation of chains of recrystallized grains takes place in the regions of former twins (Fig. 4(d)). An average

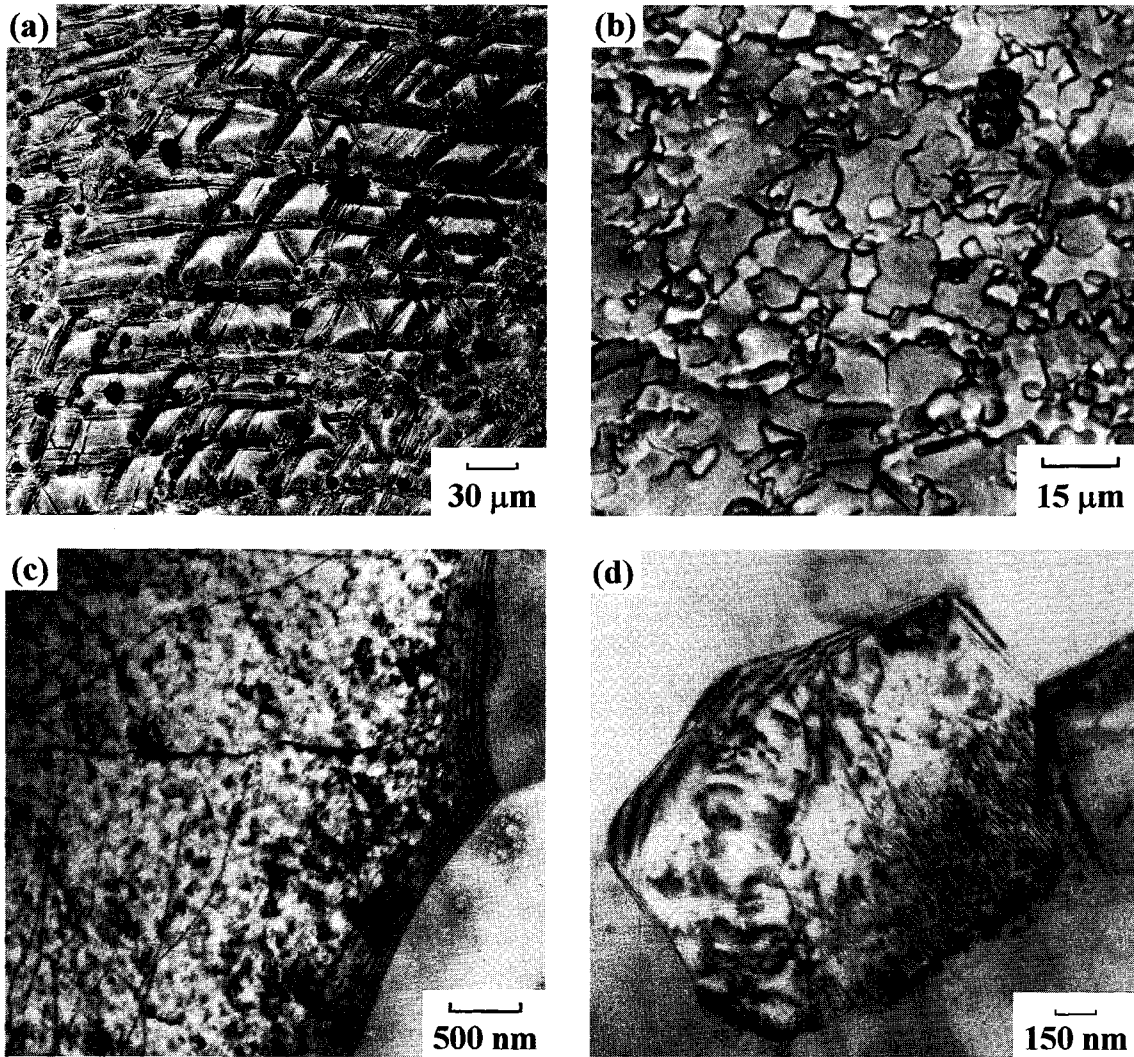


Fig. 2 Microstructures evolved in magnesium deformed by torsion under high pressure to various strains at ambient temperature. (a)  $\varepsilon = 1$ , (b, c)  $\varepsilon = 4$ , and (d)  $\varepsilon = 7$ .

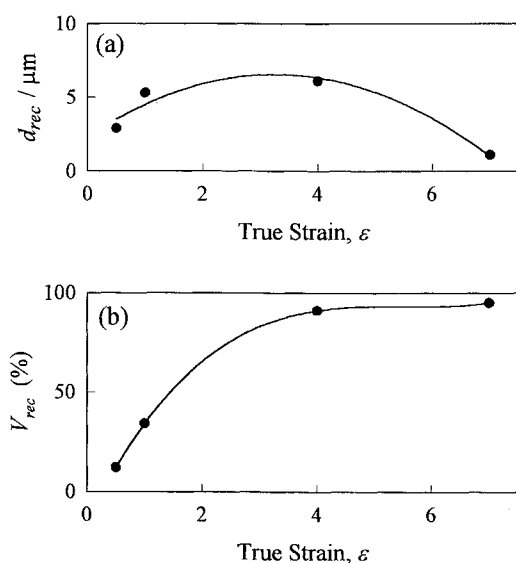


Fig. 3 Strain dependence of (a) the average recrystallized grain size,  $d_{rec}$ , and (b) the volume fraction of recrystallized grains,  $V_{rec}$ , evolved by torsion under high pressure at ambient temperature.

size of such recrystallized grains corresponds to an average width of twin lamellas. A slight growth of twin grains, which provides their equiaxed shape, occurs during following deformation.<sup>12)</sup> However, an increase in mean recrystallized grain size with strain (Fig. 5(a)) can be caused mainly by concurrent operation of CDRX mechanism.

In vicinity of initial grain boundaries the dislocation pile-ups were observed at  $\varepsilon = 0.1$  (Fig. 4(e)). The lattice dislocation densities in the mantle regions ( $\rho = 10^{14} \text{ m}^{-2}$ ) are higher than those in the grain interiors ( $\rho = 10^{13} \text{ m}^{-2}$ ). As a result, subgrain structure is formed in the mantle region.<sup>2,19)</sup> After  $\varepsilon = 0.2-0.3$ , the chains of recrystallized grains are evolved along initial grain boundaries (Fig. 4(f)). The average size of CDRX grains is larger by a factor of 1.7 than that of twin grains<sup>10)</sup> at  $\varepsilon = 0.2-0.3$ . The formation of CDRX grains is observed at higher strains than that for the twin grains. As a result, the average size of recrystallized grains tends to increase from a mean twin grain size to that of CDRX grains with increasing strain from  $\varepsilon = 0.1$  to  $\varepsilon = 1.4$ <sup>10)</sup> (Fig. 5(a)). Notably, the formation of CDRX grains was also observed near some former twin boundaries at  $\varepsilon > 0.5$ .<sup>10)</sup> A progressive increase in the volume fraction of recrystallized grains

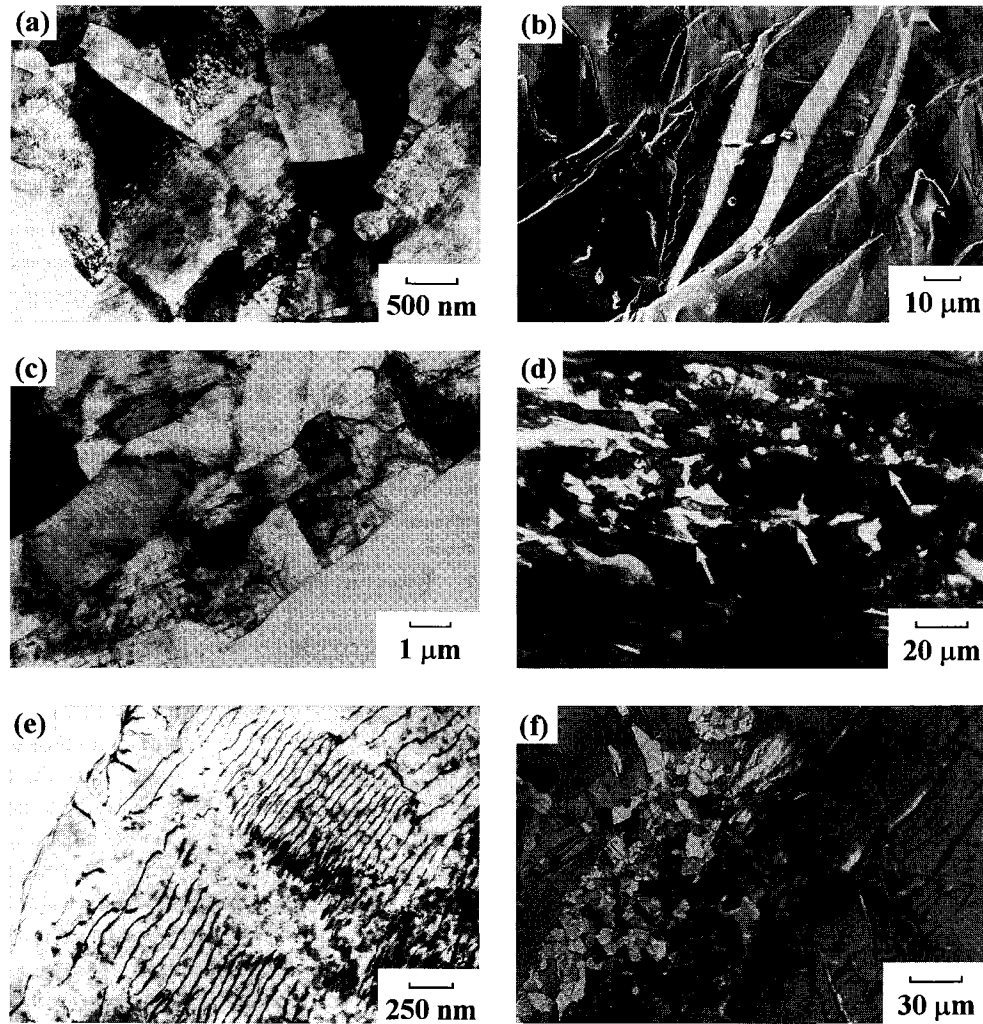


Fig. 4 Microstructure of magnesium deformed to various strains at  $T = 573$  K, (a, b, c)  $\epsilon = 0.15$ , (d)  $\epsilon = 0.7$  (arrows indicate former twin parts), (e)  $\epsilon = 0.15$ , and (f)  $\epsilon = 0.7$ .

occurs in the strain interval 0.1–0.7 (Fig. 5(b)), where CDRX and TDRX concurrently operate. A slight increment of the recrystallized volume fraction takes place at higher strains (Fig. 5(b)), where only CDRX occurs. Such microstructural evolution and strain effect on recrystallized grain size take place in the temperature interval of 523–623 K.<sup>10,18</sup> This is a range of warm plastic deformation in magnesium.<sup>15–17</sup>

### 3.3 High temperature

No deformation twinning occurred at  $T = 723$  K. A rapid growth of the volume fraction of twins up to 30 pct at  $\epsilon = 0.1$  mainly takes place due to extensive migration of initial twin boundaries (Fig. 6(a)). It can be clearly seen that twin boundaries become wavy and corrugated. An evidence for extensive migration of prior twin boundaries during following deformation was observed by polarized microscopy.<sup>10</sup> It is known,<sup>12</sup> that such twin growth can occur by migration of incoherent segments of twin boundaries, and leads to increase in the average width of twin lamellas up to 50  $\mu\text{m}$  at  $\epsilon = 0.1$ –0.15. The subdivision of the twin lamellas occurs by formation of transverse subboundaries.<sup>10,12</sup> As a result, the nuclei surrounded by a pair of twin boundaries and by a pair of low-angle boundaries are formed. These nuclei exhibit rectangular shape and

their sizes are in proportion to width of twin lamellas. After  $\epsilon = 0.3$ , first new grains exhibiting irregular shape are evolved in the sites of former twins and they comprise half of overall recrystallized grains at  $\epsilon = 0.5$ .<sup>12</sup> These twin grains are fully developed at around  $\epsilon = 0.7$ .

The formation of recrystallized grain chains evolved by CDRX<sup>10</sup> occurs along both the initial grain boundaries and the boundaries of twin grains.<sup>10</sup> These grains comprise mantle of recrystallized grains (Fig. 6(b)). The mantle fraction tends to increase with increasing strain. The formation of recrystallized grains along the initial grain boundaries begins to occur at lower strains (even at  $\epsilon = 0.1$ –0.15) and the rate of this process is higher than that along prior twin boundaries.<sup>10</sup> It is worth to note that at  $T = 723$  K the average size of twin grains is larger than that of CDRX grains.<sup>10</sup> Since twin grains are formed and grow extensively only in early stages of plastic deformation, an increase in the mean size of recrystallized grains takes place with increasing strain in the region of  $\epsilon < 0.5$  (Fig. 5(a)). A subsequent decrease in the average size of recrystallized grains (at  $\epsilon = 0.5$ –1.4) is mainly caused by refinement of coarse twin grains due to repetitive formation of recrystallized grains by CDRX mechanism.<sup>10</sup>

Additionally, a repetitive DRX, which takes place in coarse

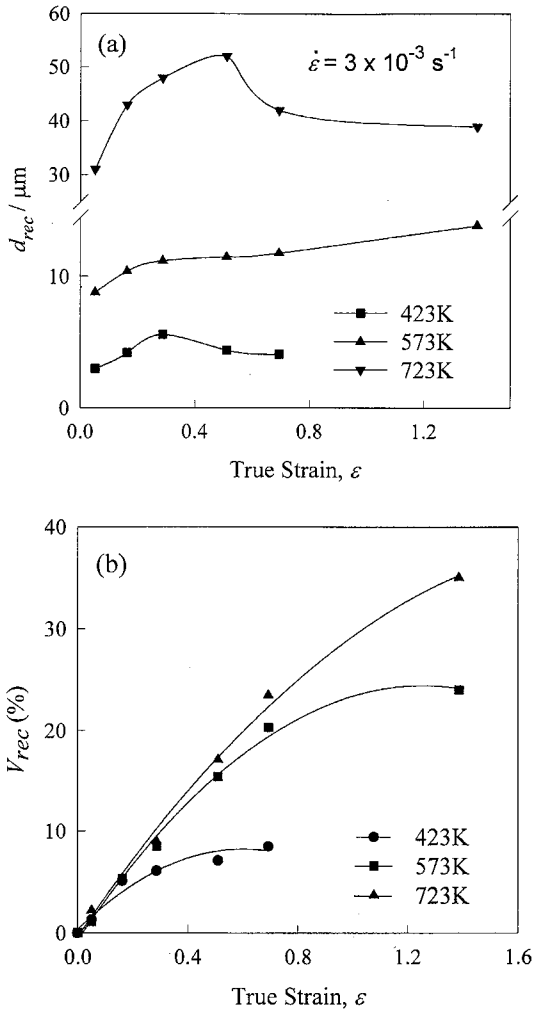


Fig. 5 Strain dependence of (a) the average recrystallized grain size,  $d_{rec}$ , and (b) the volume fraction of recrystallized grains,  $V_{rec}$ , in the temperature interval 573–723 K.

twin grains at  $\epsilon > 0.7$ , occurs also by mechanism associated with local migration of high-angle boundaries (Fig. 6(c)). This can be discontinuous DRX (DDRX). Firstly, the bulging of parts of grain boundaries are developed. With increasing strain these regions of bulging are cut off the grain matrix by development of low-angle boundaries.<sup>14</sup> These boundaries convert into high-angle boundaries with following straining and then eventually new recrystallized grains are formed. There is, however, a poor evidence for operation of such DRX mechanism in vicinity of initial grain boundaries. Repetitive DRX results in a gradual decrease in recrystallized grain size in the strain interval of 0.7–1.4. The volume fraction of recrystallized grains gradually increases with increasing strain (Fig. 5(b)). This type of microstructural evolution was observed in magnesium in the temperature range of 673–773 K, which is corresponding to a range of hot deformation in magnesium.<sup>16,17)</sup>

#### 4. Effect of Temperature and Strain on DRX

It can be concluded from the results and analysis mentioned above that four different DRX mechanisms operate in commercial grade pure magnesium in dependence on temperature and strain.<sup>10</sup> Figure 7 represents a map of DRX mechanisms operating in magnesium. Some unusual strain dependence of recrystallized grains (Figs. 3 and 5) is caused by changes in contributions of different DRX mechanisms into total recrystallization process.<sup>10,11,19</sup> As a normal rule, no strain effect on recrystallized grain size takes place during DRX.<sup>1</sup> It seems that in such cases the grain refinement occurs due to the operation of a single DRX mechanism.

Temperature dependence of the contribution of TDRX and CDRX into total recrystallization process causes an unusual temperature dependence of the volume fraction of recrystallized grains (Fig. 8(a)). In the temperature range 423–573 K

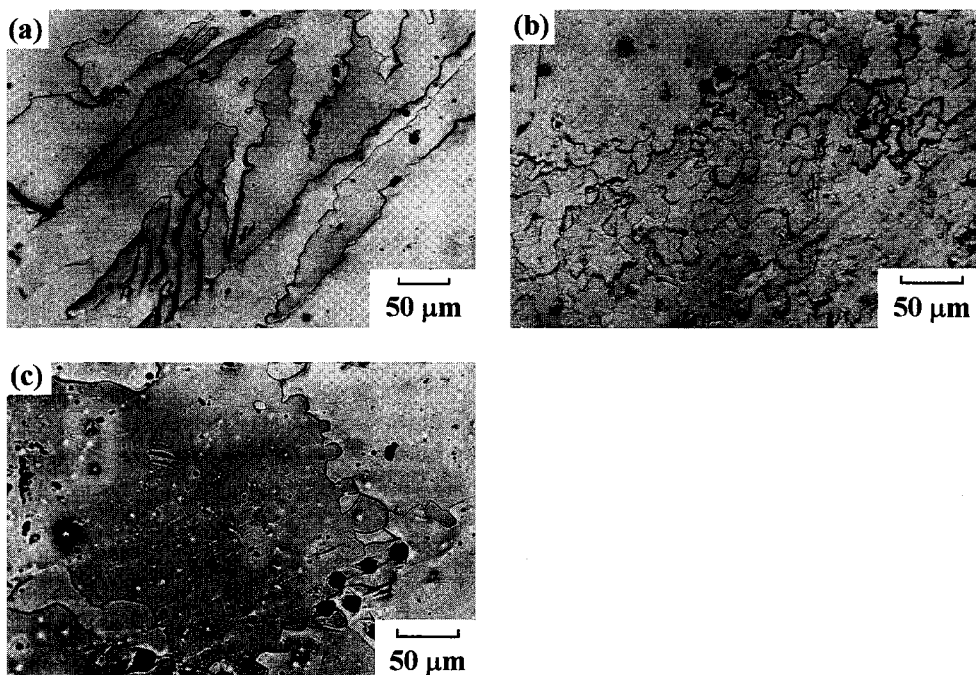


Fig. 6 Microstructures of magnesium deformed to various strains at  $T = 723 \text{ K}$ . (a)  $\epsilon = 0.1$ , (b)  $\epsilon = 0.3$ , and (c)  $\epsilon = 1$ .

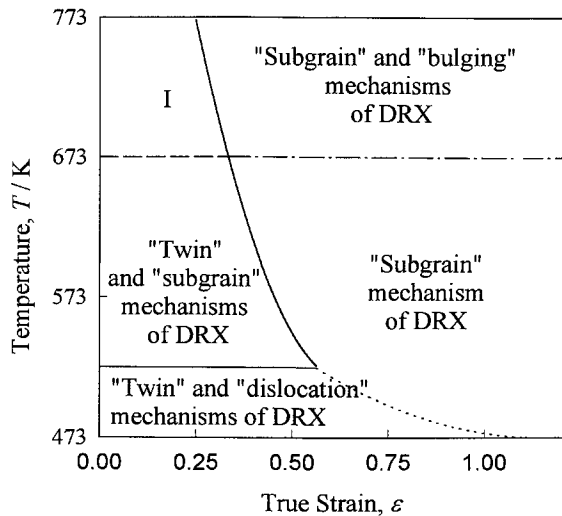


Fig. 7 A microstructural mechanism map for magnesium deformed at temperatures ranging from 293 to 773 K. I - the area, where initial twins transform into recrystallized grains during deformation.

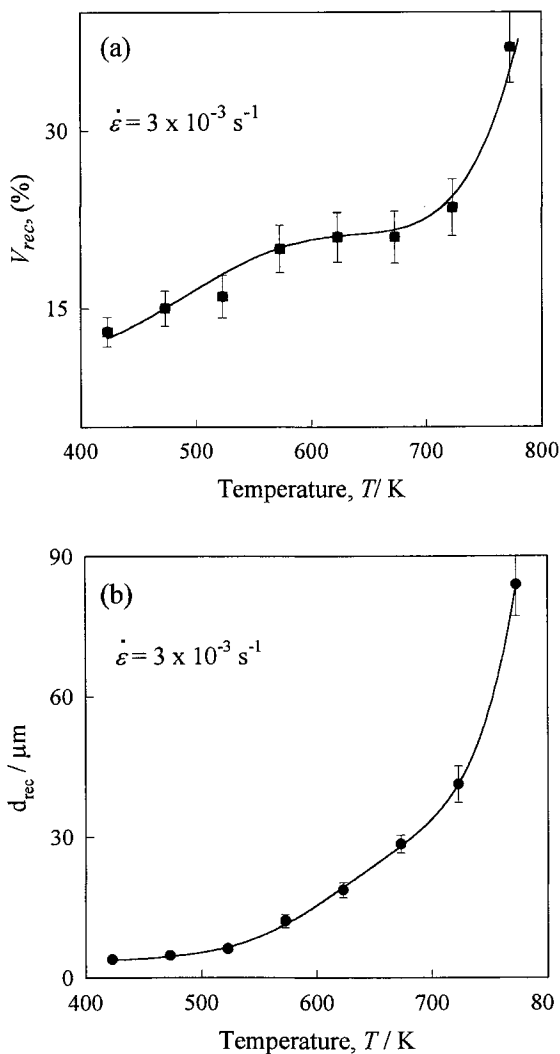


Fig. 8 Temperature dependence of characteristics of recrystallized structure at a strain of 0.7 and a strain rate of  $3 \times 10^{-3} \text{ s}^{-1}$ . (a) Volume fraction of recrystallized grains  $V_{rec}$ ; and (b) recrystallized grain size  $d_{rec}$ .

the TDRX takes place frequently with increasing temperature and a gradual increase in the volume fraction of recrystallized grains occurs. In the temperature range 573–673 K the contribution of TDRX into total recrystallization process tends to decrease and the contribution of CDRX increases with increasing temperature. As a result, the volume fraction of recrystallized grains is independent on temperature at a fixed strain. At  $T = 673\text{--}773 \text{ K}$ , a rate of CDRX increases with increasing temperature and the volume fraction of recrystallized grains increases. The size of recrystallized grains gradually increases with increasing temperature (Fig. 8(b)).

## 5. Surface observations

The surface features of strained magnesium were found to be strongly dependent on temperature. Single slip occurs mainly at low temperatures<sup>16)</sup> (Fig. 9(a)). Long slip lines are crossed in grain interiors. Multiple slip systems are operative at  $T = 523 \text{ K}$ , in some grains (Fig. 9(b)), however, only single slip takes place in most of the grains at this temperature. At  $T = 573 \text{ K}$ , wavy slip lines associated with cross-slip operation appear in the vicinity of initial boundaries (Fig. 9(c)). These lines are essentially short. Their mean size is about  $1 \mu\text{m}$ . Extensive deformation twinning takes place at temperatures ranging from 293 to 623 K (Fig. 4(b)).<sup>12, 16)</sup> At  $T = 723 \text{ K}$ , cross-slip predominantly occur (Fig. 9(d)). Long and wavy lines of basal slip propagate through whole grain areas and twin lamellas. Intersection of these slip lines with twin boundaries brings about a change in their direction (Fig. 9(d)). Therefore, mobile dislocations can glide through grain boundaries in basal plane. Extensive non-basal slip occurs both in the vicinity of initial boundaries (Fig. 9(e)) and twin boundaries (Fig. 9(d)).

Figure 10 summarizes the deformation mechanisms in the magnesium on the base of surface observation and analysis of mechanical data.<sup>16, 17)</sup> It is seen that a temperature increase hinders deformation twinning and facilitates operation of cross-slip and dislocation slip on multiple systems. At elevated temperatures cross-slip occurring in accordance either with Fridel–Esaig or Fridel mechanism<sup>17)</sup> can be a rate-controlling process.

## 6. DRX Mechanisms in Magnesium

### 6.1 TDRX mechanism

Some DRX mechanisms associated with twinning play an important role in plastic deformation of magnesium. TDRX mechanism involves the three elementary processes: *i.e.* nucleation, transformation of twin boundaries into random boundaries and grain growth (Fig. 11).<sup>12)</sup> Three nucleation mechanisms can operate; namely.

- Mutual intersection of primary twins results in the formation of crystallites surrounded by twin boundaries (Figs. 2(a), 4(a), 11(a)).
- The other nuclei can be formed as a result of secondary twinning within primary twin lamellas (Figs. 4(b) and 11(b)). These nucleation mechanisms are associated with deformation twinning.
- In addition, deformation or annealing twins can be subdivided into nuclei by development of transverse

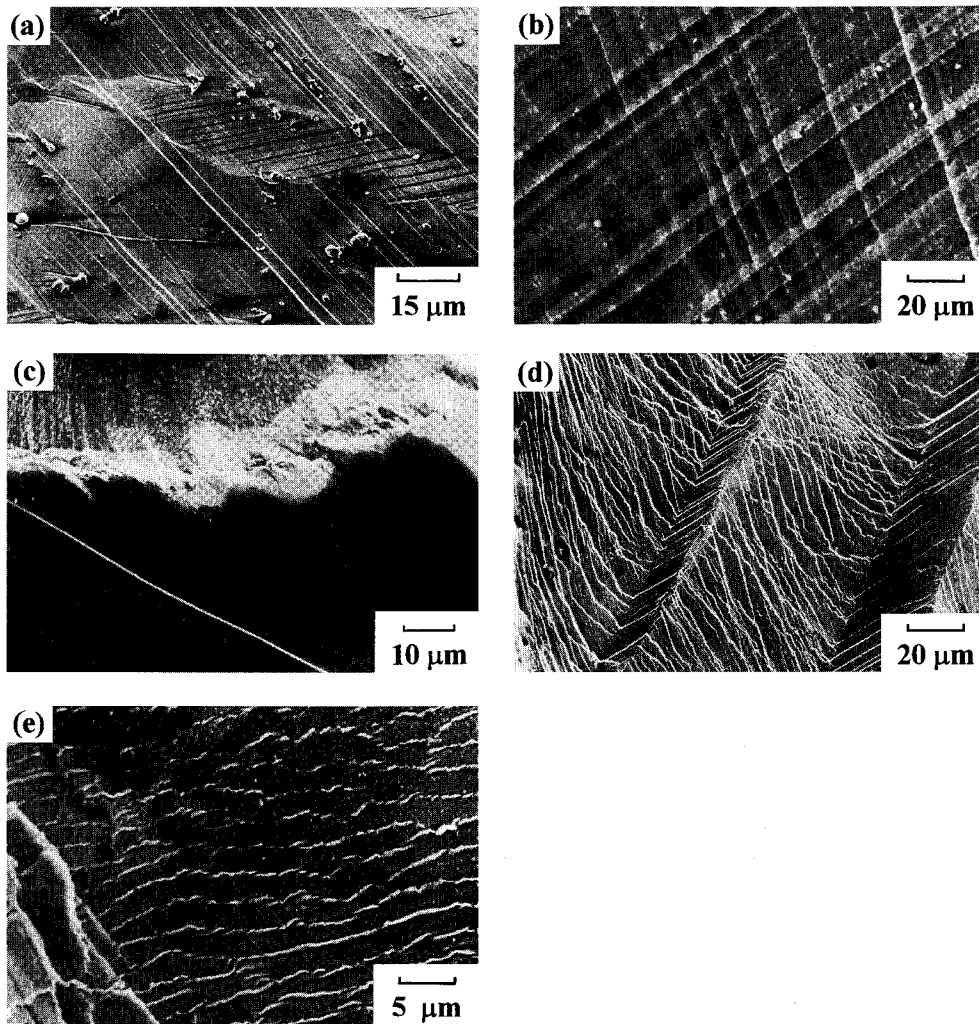


Fig. 9 Surface observations of magnesium deformed to a strain of 0.15 at  $\dot{\epsilon} = 3 \times 10^{-3} \text{ s}^{-1}$ . (a)  $T = 423 \text{ K}$ , (b)  $T = 523 \text{ K}$ , (c)  $T = 573 \text{ K}$ , and (d), (e)  $T = 723 \text{ K}$ .

low-angled boundaries (Figs. 4(c) and 11(c)).

The second stage of TDRX mechanism is to transform twin boundaries into high angle random boundaries due to deviation of misorientation angle from coincident site lattice relationship on a value over than the standard Brandon criteria.<sup>20)</sup> This transformation can result from the formation of misfit dislocations comprising a dislocation wall. This wall provides a change in misorientation angle of coherent twin boundaries, which transform into random boundaries due to an additional increase in the misorientations. Misfit dislocations ( $b_3$  and  $b_4$  in Fig. 11(d)) are formed to compensate the change in the dislocation glide direction, when a lattice dislocation intersects a twin boundary and passes from matrix grain to twinned area (Fig. 9(d)). Transverse subboundaries in coarse twin lamellas transform to high-angle boundaries by CDRX mechanism, which will be discussed in next paragraph.

Random boundaries have a high ability of migration and are not transparent for mobile lattice dislocations. Migration of such boundaries leads to the elimination of large number of lattice dislocations. Thus, TDRX gives a significant contribution in strain softening taking place during deformation in the range of low and intermediate temperatures. An apparent steady-state flow at  $T = 293 \text{ K}$  and steady-state defor-

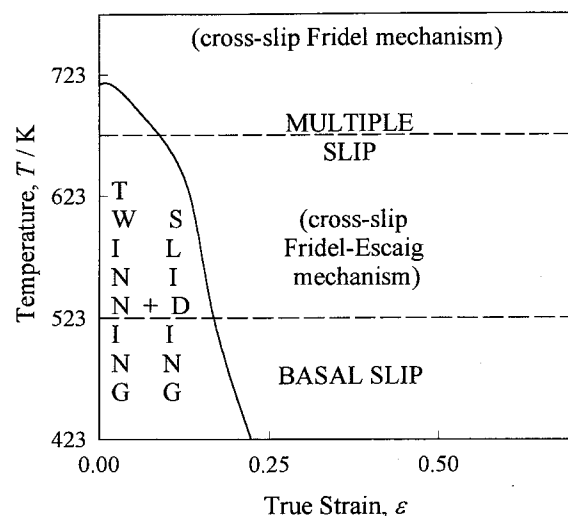


Fig. 10 A map of deformation mechanisms operating in Mg. Controlling mechanisms of plastic deformation are indicated in brackets.

mation at temperatures ranging from 423 to 623 K are established by TDRX. Moreover, an extensive migration of former twin boundaries results in the formation of equiaxed twin

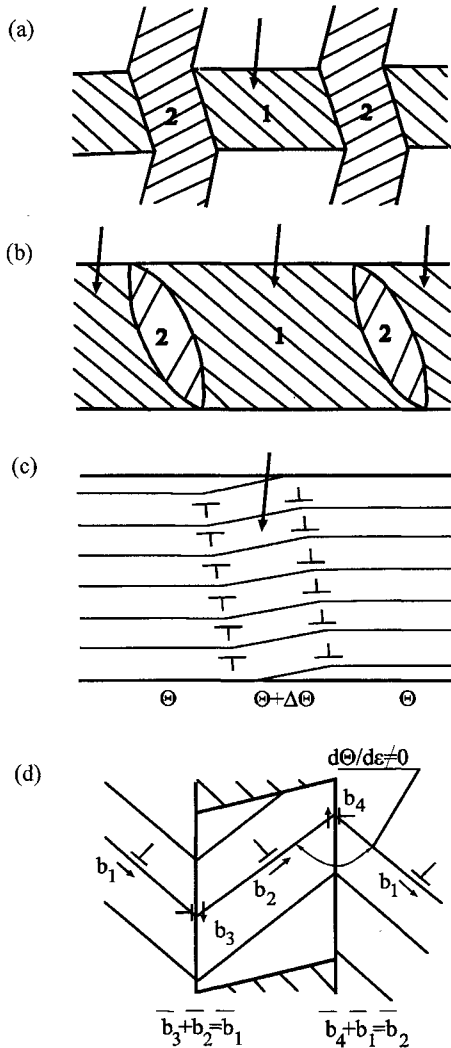


Fig. 11 Schematic representation of "twin" DRX mechanism.<sup>12)</sup> (a) Nucleation by mutual intersection of primary twins 1 and 2; (b) nucleation by subdivision of coarse primary twin lamellas 1 by fine secondary twins 2; (c) nucleation by subdivision of primary twin lamellas by transverse low-angle boundaries; and (d) scheme of formation of orientation misfit dislocations (with Burger's vectors  $b_3$  and  $b_4$ ) in twin boundaries providing a change in misorientation of twin boundaries.

grains with triple junction angles close to  $120^\circ$ .<sup>12)</sup> Random twin boundaries can play a role in the operation of CDRX.

## 6.2 CDRX in magnesium

Occurrence of CDRX can be attributed with dislocation slip in the mantle regions of initial grains. Surface observations<sup>10,12,16)</sup> and analysis of Burgers vectors of lattice dislocations<sup>2)</sup> showed that multiple slip occurs near initial boundaries and former twin boundaries. Only rearrangement of lattice dislocations belonging to different slip systems can result in the formation of low-angle boundaries.<sup>21)</sup> In addition, high density lattice dislocations sufficient for subgrain formation are accumulated only near random high-angle boundaries. Thus, subgrains predominantly form in the mantle regions.

It is known that cross-slip of lattice dislocations is the slowest process of dislocation rearrangement in magnesium.<sup>22)</sup> As a result, this process is a rate controlling process of plastic

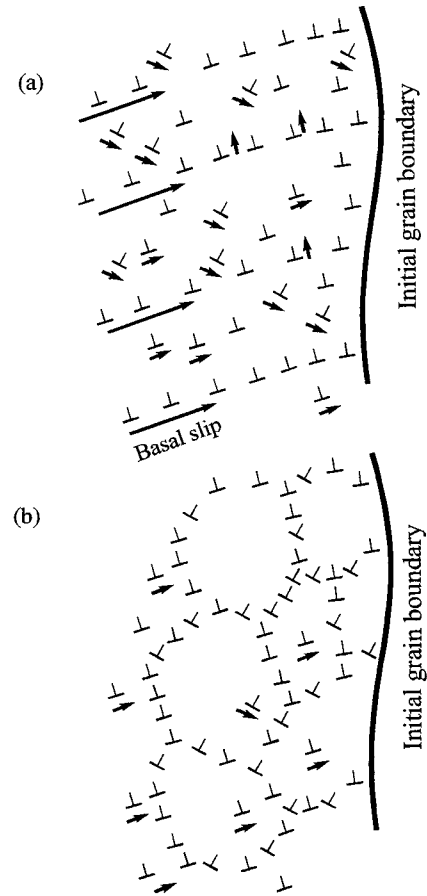


Fig. 12 Schematic representation of continuous DRX mechanism. (a) Dislocation pile-ups in the vicinity of initial grain boundary; and (b) nucleation and gradual increase of misorientation of subboundary due to trapping mobile dislocations.

deformation at intermediate and high temperatures,<sup>16,17)</sup> and also can control the rate of subgrain formation. It is known that SFE in the first order pyramidal and prismatic planes of magnesium is higher by a factor of 4 than that in the basal plane.<sup>5,6)</sup> Dislocations of non-basal slip systems, therefore, can easily recombine and cross-slip, as these are suggested by surface observations. In addition, our examinations of deformation mechanisms<sup>16,17)</sup> showed that SFE in the basal plane of magnesium is about  $40 \text{ MJ/m}^2$ . As a result, dislocations belonging to the basal system also exhibit ability to cross-slip at high temperatures, as this is evident by direct observations (Fig. 9(d)).

It was shown that  $\alpha$ -dislocations lying in the basal plane generally rearrange into tilt boundaries perpendicular to basal planes<sup>2)</sup> (Figs. 12(a), (b)). Deformation induced subboundaries evolved in the basal plane consist of dislocations belonging to non-basal slip systems. Two pairs of low-angle boundaries comprising of basal and non-basal dislocations are required for the formation of a two dimensional nucleus. Formation of twist boundaries consisting of dislocations belonging to non-basal slip systems may be a slowest process, and control nucleation. Thus, CDRX mechanism typically observed in materials with high SFE occurs in the magnesium.

Mobile dislocations introduce subboundaries evolved dur-



ing following deformation (Fig. 12(b)). The trapping of lattice dislocations by low-angle boundaries results in gradual increase in their misorientation. Transformation of low-angle boundaries into high-angle ones takes place with strain. Following migration of high-angle boundaries provides equiaxed shape of recrystallized grains. CDRX can result in a strain softening followed by a steady-state flow in the range of intermediate and high temperature.

### 6.3 “Bulging” mechanism of DRX

It was shown<sup>14)</sup> that DRX mechanism associated with local migration of initial boundaries is operative in grains having optimal localization of dislocation glide at high temperatures. The latter is a necessary condition for operation of bulging process (Fig. 13(a)).<sup>14)</sup> In pure magnesium the local migration of boundary occurs toward areas with high density dislocations, leading to the development of grain boundary irregularities. It is known<sup>2,7,8)</sup> that grain boundary sliding taking place on such non-planar boundaries can result in strong strain gradient near the boundaries (Fig. 13(b)). Accommodation of plastic deformation is provided by operation of grain boundary dislocation sources, which emit dislocations into grain interiors (Fig. 13(b)). These dislocations usually belong to non-basal systems.<sup>14)</sup> Interaction of these dislocations with basal dislocations yields the formation of subboundaries, which cut off the protrusion from the grain body (Fig. 13(c)). The misorientation of such subboundaries

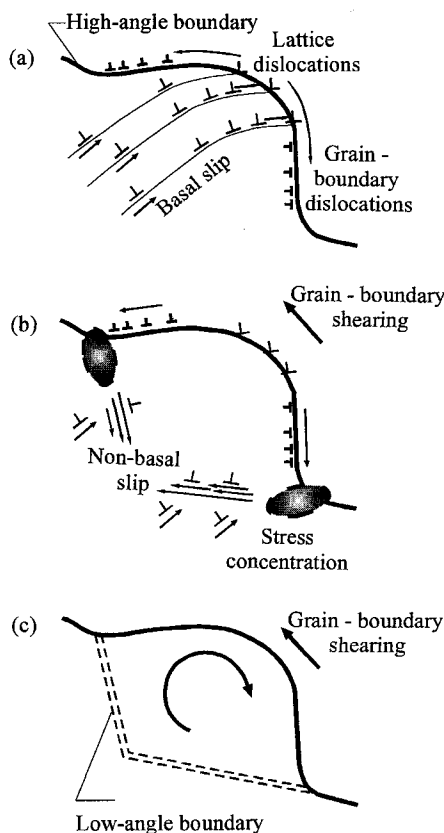


Fig. 13 Schematic representation of “bulging” DRX.<sup>14)</sup> (a) Local migration of boundary toward slip localization in magnesium, (b) partial grain boundary shearing, leading to the development of inhomogeneous strain gradients and cutting of protrusion by a multiple slip band, and finally (c) formation of medium to high angle boundaries at the place of bulging out.

gradually increases with increasing strain due to trapping of lattice dislocations (Fig. 12(b)), finally leading to the development of high-angle boundaries. The DDRX is assisted by operation of grain boundary sliding<sup>2,7,8)</sup> and, therefore, can take place frequently with increasing temperature.

### 6.4 LTDRX mechanism

High density dislocation pile-ups are formed in fine grains resulted from TDRX. It provides a strong bending of crystal lattice. Examination of LTDRX mechanism is in progress, but it is possible to assume that grain boundaries can be evolved as a result of local planar dislocation accumulation. This accumulation provides a decrease in energy of dislocation system. Short-range dislocation rearrangements yield a boundary containing high density grain boundary dislocations.<sup>13)</sup> Long-range stress fields originated from these dislocations causes a bending of crystal lattice within grains evolved.<sup>23,24)</sup> As a result, a strong increase in internal elastic strain and, consequently, microhardness is observed during LTDRX.

## 7. Deformation Mechanisms and DRX

Analysis of the deformation mechanism map (Fig. 10) in conjunction with microstructural mechanism map (Fig. 7) allows establishing a strong correlation between DRX mechanisms and operating deformation mechanisms. This is caused by the fact that a specific mechanism of plastic deformation can result in a respective DRX mechanism. Thus, such features of recrystallization behavior of the magnesium, namely in the strain dependence of recrystallized grain size (Figs. 3(a) and 5(a)) and the unusual temperature dependence of recrystallized volume fraction (Fig. 8(a)), are caused by effects of temperature and strain on operating deformation mechanisms, which are closely related with the mechanisms of DRX nucleation.

In support to this conclusion, Fig. 14 represents a relationship between dynamic grain size evolved and flow stress at high strains. It is seen that a transition in DRX mechanisms results in a change of the slope of the relationship of  $\sigma \sim d_{rec}^{-N}$ , where  $\sigma$  is the flow stress,  $d_{rec}$  is the recrystallized grain size and  $N$  is a constant. It is seen clearly in Fig. 14 that two linear relationships of  $\sigma \sim d_{rec}^{-N}$  can result from different dynamic grains evolved by LTDRX and CDRX mechanisms.

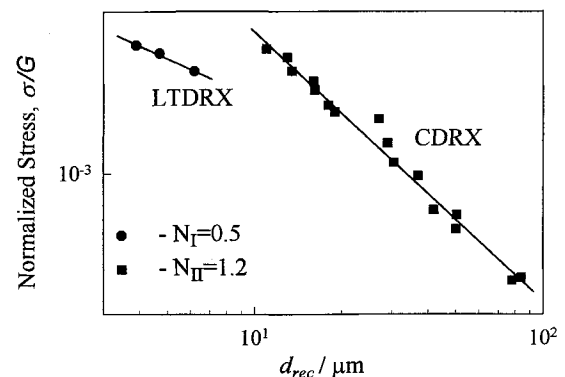


Fig. 14 Relationship between normalized applied stress,  $\sigma/G$ , and average recrystallized grain size,  $d_{rec}$ , in magnesium. The grain sizes evolved by LTDRX and CDRX was taken into account.

## 8. Conclusions

(1) DRX occurs in coarse-grained pure magnesium in the wide temperature range 293–773 K. Three temperature ranges, namely the low temperature interval 293–473 K, the intermediate temperature interval 523–623 K and the high temperature interval 673–773 K, can be distinguished by characteristics of microstructural evolution.

(2) It is concluded that the four different mechanisms of DRX nucleation and the operating deformation mechanisms are closely related. Twin DRX is associated with mechanical twinning at low and intermediate temperatures, and transformation of annealing twin lamellas at the high temperatures. This mechanism plays an important role in the strain interval of 0.1–4 and processes material softening at  $T = 293$ –623 K. Continuous DRX takes place during steady-state flow in the temperature range of 523–773 K. This DRX mechanism is related with operation of cross-slip on multiple systems near high angle boundaries. CDRX plays an important role in the establishment of steady-state flow in the ranges of intermediate and high temperatures. Discontinuous DRX plays a minor role of a repetitive DRX mechanism at high temperature and associated with localization of dislocation glide. Mechanism of low temperature DRX results in the formation of grains with a mean size of about 1  $\mu\text{m}$  at ambient temperature. LTDRX occurs due to low ability of lattice dislocations to rearrange and yields strain hardening.

(3) Temperature dependence of recrystallized grain size can be caused by changes in contribution of different DRX mechanisms in total microstructural evolution with increasing temperature.

(4) Different strain dependencies of recrystallized grain size in the three different temperature intervals can be caused by changes in contribution of different DRX mechanisms in total microstructural evolution with increasing strain at the three different temperature regions.

## Acknowledgements

One of authors (R.K.) would like to express his hearty thanks to the Japan Society for the Promotion of Science for providing scientific fellowship.

## REFERENCES

- 1) T. Sakai and J. J. Jonas: *Acta Metall.* **32** (1984) 189–209.
- 2) S. E. Ion, F. J. Humphreys and S. H. White: *Acta Metall.* **30** (1982) 1909–1919.
- 3) O. Sivakesavam, I. S. Rao and Y. V. R. K. Prasad: *Mater. Sci. Technol.* **9** (1993) 805–810.
- 4) S. Gourdet and F. Montheillet: *Mater. Sci. Eng. A* **283** (2000) 274–288.
- 5) B. Legrand: *Philos. Mag. A* **49** (1984) 171–179.
- 6) M. Igarashi, M. Khantha and V. Vitek: *Philos. Mag. A* **63** (1991) 603–627.
- 7) A. Belyakov, H. Miura and T. Sakai: *Mater. Sci. Eng. A* **255** (1998) 139–147.
- 8) H. Miura, H. Aoyama and T. Sakai: *J. Jpn. Inst. Metals* **58** (1994) 269–275.
- 9) G. Gottstein and U. F. Kocks: *Acta Metall.* **31** (1983) 175–188.
- 10) R. Kaibyshev and O. Sitdikov: *Phys. Met. Metall.* **73** (1992) 635–642.
- 11) R. Kaibyshev and O. Sitdikov: *Z. Metallk.* **85** (1994) 738–743.
- 12) R. Kaibyshev and O. Sitdikov: *Phys. Met. Metall.* **89** (2000) 384–390.
- 13) M. Mabuchi, K. Ameyama, H. Iwasaki and K. Higashi: *Acta Mater.* **47** (1999) 2047–2057.
- 14) R. Kaibyshev and O. Sitdikov: *Phys. Met. Metall.* **78** (1994) 420–427.
- 15) R. Kaibyshev and O. Sitdikov: *Physics-Doclady* **38** (1993) 475–478.
- 16) R. Kaibyshev and O. Sitdikov: *Phys. Met. Metall.* **80** (1995) 354–360.
- 17) R. Kaibyshev and O. Sitdikov: *Phys. Met. Metall.* **80** (1995) 470–475.
- 18) R. Kaibyshev and O. Sitdikov: *DAN, Physics-Doclady* **321** (1991) 306–310.
- 19) N. Zaripov, A. Vagapov and R. Kaibyshev: *Phys. Met. Metall.* **63** (1987) 774–781.
- 20) O. Kaibyshev and R. Valiev: *Grain Boundaries and Properties of Metals*, (Metallurgy, Moscow, 1987) p. 214.
- 21) M. A. Shtremel: *Strength of alloys. Lattice defects*, (MSAI, Moscow, 1999) p. 547.
- 22) A. Couret and D. Caillard: *Acta Metall.* **33** (1985) 1447–1462.
- 23) A. Belyakov, T. Sakai, H. Miura and R. Kaibyshev: *Scr. Mater.* **42** (2000) 319–325.
- 24) A. Belyakov, T. Sakai, H. Miura and R. Kaibyshev: *Philos. Mag. Lett.* **80** (2000) 711–718.